DALTON
FULL PAPER

Coordination chemistry of a bulky redox-active cyanomanganese carbonyl ligand: *N*-bound tetrahedral complexes of 3d metals

Neil G. Connelly,* Owen M. Hicks, Gareth R. Lewis, A. Guy Orpen and Andrew J. Wood

School of Chemistry, University of Bristol, Bristol, UK BS8 1TS.
E-mail: Neil.Connelly@bristol.ac.uk

Received 6th March 2000, Accepted 31st March 2000

The sterically hindered redox-active cyanomanganese carbonyl complex *trans*-[Mn(CN)(CO)(dppm)$_2$] acts as an *N*-donor ligand towards MCl_2 (M = Mn, Co or Ni) to give the cyanide-bridged tetrahedral (at M) complexes [Cl_2(thf)M(μ-NC)MnL_x] {L_x = (CO)(dppm)$_2$}. Displacement of the labile thf ligand by chloride ion affords anionic [Cl_3M(μ-NC)MnL_x]$^-$ which is oxidised to [Cl_3M(μ-NC)MnL_x], containing two paramagnetic centres, tetrahedral M(II) and low spin octahedral Mn(II). The cobalt(II) complex [Cl_2(thf)Co(μ-NC)MnL_x] also undergoes thf substitution with neutral *N*-donor ligands to give [Cl_2L′Co(μ-NC)MnL_x] {L′ = 4,4′-bipy or (NC)Mn(PPh_3)(NO)(η-C_5H_4Me)}; the latter is oxidised to the mixed valence trimetallic cation [Cl_2Co^{II}{(μ-NC)$Mn^{II}L_x$}{(μ-NC)Mn^{I}(PPh_3)(NO)(η-C_5H_4Me)}]$^+$. X-Ray structural studies on [Cl_2(thf)M(μ-NC)MnL_x] (M = Co, Mn or Ni) and [Cl_3Mn(μ-NC)MnL_x] show distortion of the M–N–C angle to accommodate non-bonded interactions between the phenyl groups of the bulky Mn(dppm)$_2$ moiety and the ligands at the tetrahedral metal; distortions of the tetrahedral valence angles at the M^{II} centres of [Cl_2(thf)M(μ-NC)MnL_x] may in part be related to the weak binding of thf.

Introduction

Cyanide-bridged complexes with the Mn^{I}(μ-CN)M core, systematically constructed by attaching redox-active, *N*-donor manganese(I) 'ligands' such as *trans*-[Mn(CN)(CO)(dppm)$_2$],[1] *cis*- and *trans*-[Mn(CN)(CO)$_2${P(OR)$_3$}(dppm)] (R = Et or Ph)[2] and [Mn(CN)(PR_3)(NO)(η-C_5H_4Me)] (R = Ph or OPh)[3] to a second metal centre, M, show electron transfer behaviour and other electronic properties[4,5] which are influenced by the coordination geometry and ancillary ligands at both Mn(I) and M. To date, most of our studies have involved transition metals, M, in low oxidation states, such as linear gold(I),[6] square planar Rh(I),[7] tetrahedral Fe(−I),[8] *etc*. However, preliminary studies showed[9] that cyanomanganese ligands could also coordinate to first row transition metal dihalides MCl_2 (M = Mn, Co and Ni) to give bi- and poly-nuclear species in which an organometallic fragment, *i.e.* a low spin carbonylphosphinemanganese(I) centre, is *N*-bonded to a classical coordination complex centre, such as tetrahedral M^{II}. (Some similar chemistry has since been demonstrated by Vahrenkamp using the ligand [Fe(CN)(dppe)(η-C_5H_5)].[10]) We now give details of the reactions of MCl_2 (M = Mn, Co and Ni) with the bulky ligand *trans*-[Mn(CN)(CO)(dppm)$_2$] which lead to the isolation of [Cl_2(thf)M(μ-NC)MnL_x],† precursors to a range of hetero-bi- and tri-nuclear cyanide-bridged complexes by virtue of the easily replaced thf co-ligand at M.

Results and discussion

Synthesis

The reaction of one equivalent of *trans*-[Mn(CN)(CO)(dppm)$_2$] with $CoCl_2$·6H_2O (in acetone) or MCl_2 (M = Mn or Ni) (in EtOH–thf) gave the air-stable heterobimetallic complexes [Cl_2(thf)M(μ-NC)MnL_x] {M = Co (**1**), Mn (**2**) or Ni (**3**)}

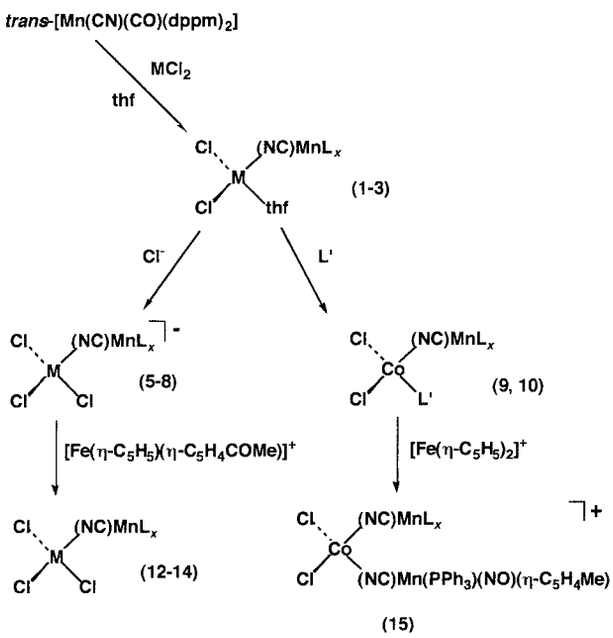

Scheme 1 L_x = (CO)(dppm)$_2$; M = Co, Mn or Ni.

(Scheme 1) after filtration and evaporation of the reaction mixture to dryness, extraction of the residue into thf and addition of *n*-hexane to the filtered extract. Reproducible synthetic routes to higher nuclearity complexes, *i.e.* by the displacement of thf from **1**–**3** using an excess of *trans*-[Mn(CN)(CO)(dppm)$_2$], were not found, in contrast to the formation of [Cl_{4-n}M{(μ-NC)MnL_y}$_n$]$^{(n-2)+}$ (n = 1–4) where L_y = *cis*- or *trans*-(CO)$_2${P(OR)$_3$}(dppm).[9,11] {However, the crystal structure of the trimetallic complex [Cl_2Co{(μ-NC)MnL_x}$_2$] was obtained fortuitously (see below).}

If *n*-hexane was added directly to the product of the reaction between *trans*-[Mn(CN)(CO)(dppm)$_2$] and $CoCl_2$·6H_2O in acetone (*i.e.* in the absence of thf), a different green product, **4**, was obtained. Although **4** has not been structurally

† Throughout this paper the (μ-NC)Mn(CO)(dppm)$_2$ unit retains the structure in which the carbonyl ligand is *trans* to the cyanide bridge, with the cyanide group *C*-bound to Mn. The ligand set (CO)(dppm)$_2$ is abbreviated to L_x.

DOI: 10.1039/b001782p

characterised, the elemental analysis (C, H and N), the presence in the IR spectrum (Nujol mull) of a broad ν(O–H) band at *ca.* 3300 cm^{-1}, and a FAB mass spectrum showing a peak at *m/z* 1006 {corresponding to the $Cl_2Co(\mu\text{-}NC)MnL_x$ moiety}, are consistent with the formulation $[Cl_2(H_2O)Co(\mu\text{-}NC)MnL_x]$. When solid **4** was added to deoxygenated CH_2Cl_2 and the mixture stirred for *ca.* 1 h, the initial green suspension dissolved to give a brown solution. Addition of *n*-hexane under anaerobic conditions then gave an extremely reactive brown solid **A** which very rapidly gave a green powder on exposure to air or to the vapour of a coordinating solvent such as thf or water; the colour change from brown to green was reversed under vacuum. A reaction sequence which accounts for these observations is shown in Scheme 2. Elimination of water from **4** in CH_2Cl_2 and

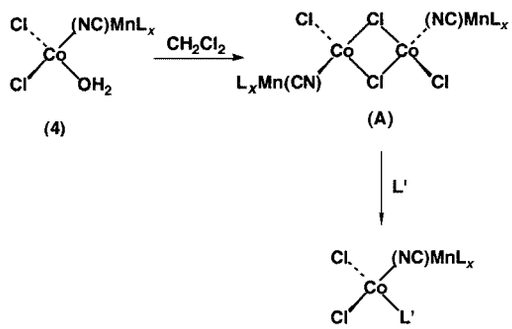

Scheme 2 L′ = solvent or water, L_x = (CO)(dppm)$_2$.

dimerisation is expected to give the brown chloro-bridged complex $[\{ClCo(\mu\text{-}NC)MnL_x\}_2(\mu\text{-}Cl)_2]$ **A** which forms the green monomer $[Cl_2L'Co(\mu\text{-}NC)MnL_x]$ on contact with a coordinating ligand, L′. Water is also displaced from **4** by layering *n*-hexane on a concentrated thf solution of **4**, giving crystals of $[Cl_2(thf)Co(\mu\text{-}NC)MnL_x]$ **1**.

Complexes **1**–**3** react with chloride ion in CH_2Cl_2 to give the anions $[Cl_3M(\mu\text{-}NC)Mn(CO)(dppm)_2]^-$, characterised as the salts $[NEt_3Bz][Cl_3Co(\mu\text{-}NC)Mn(CO)(dppm)_2]$ {$[NEt_3Bz]$[**5**] (Bz = benzyl)} or $[PPN][Cl_3M(\mu\text{-}NC)Mn(CO)(dppm)_2]$ {M = Co ([PPN][**6**]), Mn ([PPN][**7**]) or Ni ([PPN][**8**]); PPN = $[N(PPh_3)_2]^+$}. The coordinated thf of $[Cl_2(thf)Co(\mu\text{-}NC)Mn(CO)(dppm)_2]$ **1** is also replaced by 4,4′-bipyridine, forming $[Cl_2(4,4'\text{-bipy})Co(\mu\text{-}NC)Mn(CO)(dppm)_2]$ **9**. Although the pendant nitrogen atom of the 4,4′-bipyridine ligand in **9** is also available for coordination to a second metal centre, the reaction of two equivalents of **1** with one of 4,4′-bipy gave only **9**, rather than the tetrametallic complex $[(\mu\text{-}4,4'\text{-bipy})\{Cl_2Co(\mu\text{-}NC)Mn(CO)(dppm)_2\}_2]$.

With the pseudo-tetrahedral cyanomanganese ligand $[Mn(CN)(PPh_3)(NO)(\eta\text{-}C_5H_4Me)]$, complex **1** forms trimetallic $[Cl_2Co\{(\mu\text{-}NC)MnL_x\}\{(\mu\text{-}NC)Mn(PPh_3)(NO)(\eta\text{-}C_5H_4Me)\}]$ **10**. This contrasts with the absence of a rational synthesis of $[Cl_2Co\{(\mu\text{-}NC)MnL_x\}_2]$ from **1** and *trans*-$[Mn(CN)(CO)(dppm)_2]$, probably reflecting the relative sizes of *trans*-$[Mn(CN)(CO)(dppm)_2]$ and $[Mn(CN)(PPh_3)(NO)(\eta\text{-}C_5H_4Me)]$ whose cone angles as *N*-donor ligands have been estimated at 188(4) and 119° respectively.[12]

Complexes **1**–**10** have been characterised by elemental analysis, magnetic susceptibility studies and UV-visible (for cobalt) and IR spectroscopy (Tables 1 and 2). The cobalt complexes **1** and **6**, the manganese complexes **2** and **7**, and the nickel complex **3** show room temperature magnetic moments (Table 2) consistent with the presence of tetrahedral d^7,[13] d^5 [14] and d^8 M(II) centres respectively. [The magnetic moment of **3** (μ = 3.3 μ_B) is similar to those of more distorted tetrahedral Ni(II) complexes which show moments in the range 3.0–3.5 μ_B.[15]] The UV-visible spectra of solutions of **1** and **6** are also in agreement with the presence of tetrahedral Co(II) centres, with bands very similar in energy and intensity to those of $[PPN][CoCl_4]$.

Table 1 Analytical and IR spectroscopic data for $[Cl_2L'M(\mu\text{-}NC)MnL_x]$[z]

Complex	L′	M	*z*[c]	Colour	Yield (%)	Analysis[a,b] (%) C	H	N	Cl	IR[e]/cm^{-1} ν(CN)	ν(CO)
1	thf	Co	0	Green	80	62.7 (62.3)	4.5 (4.9)	1.1 (1.3)	—	2086mw[d]	1879s[d]
2	thf	Mn	0	Orange	71	62.1 (62.5)	5.0 (4.9)	1.7 (1.3)	—	2077mw[d]	1880s[d]
3	thf	Ni	0	Brown	56	62.1 (62.5)[e]	5.0 (5.3)	0.9 (1.2)	—	2098w[d]	1878s
4	H_2O	Co	0	Green	85	60.7 (60.9)	4.6 (4.5)	1.4 (1.4)	—	2083w, 2077mw[f]	1871s[f]
5	Cl	Co	−1[g]	Green	66	61.9 (61.6)	5.4 (5.3)	2.4 (2.2)	—	2089mw	1872s
6	Cl	Co	−1	Green	73	63.7 (64.1)[h]	4.9 (4.6)	1.4 (1.7)	11.0 (10.6)	2092mw	1872s
7	Cl	Mn	−1	Orange	81	65.7 (66.0)	4.6 (4.7)	2.1 (1.8)	—	2085mw	1871s
8	Cl	Ni	−1	Green	72	65.8 (65.5)[i]	4.6 (4.7)	1.9 (1.7)	8.5 (8.7)	2102mw	1868s
9	4,4′-bipy	Co	0	Green	66	63.9 (64.0)	4.5 (4.5)	3.2 (3.6)	—	2082m	1876s
10	(NC)Mn(PPh$_3$)-(NO)(η-C$_5$H$_4$Me)	Co	0	Green	53	61.7 (62.0)[i]	4.5 (4.5)	3.3 (2.8)	—	2090mw	1876s[j]
12	Cl	Co	0	Purple	85	60.0 (59.9)	3.9 (4.3)	1.3 (1.3)	—	2123mw	1945s
13	Cl	Mn	0	Dark red	70	56.7 (56.6)[h]	4.0 (4.1)	1.4 (1.3)	15.1 (15.8)	2118w	1944s
14	Cl	Ni	0	Dark red	77	57.9 (58.1)[i]	4.4 (4.2)	1.3 (1.3)	13.1 (13.1)	2131w	1943s
15	(NC)Mn(PPh$_3$)-(NO)(η-C$_5$H$_4$Me)	Co	1[k]	Blue	—	—	—	—	—	2121ms	1949s[l]

[a] Calculated values in parentheses. [b] Anions isolated as $[PPN]^+$ salts unless stated otherwise. [c] In CH_2Cl_2 unless stated otherwise; s = strong, m = medium, w = weak. [d] In thf. [e] Analysed as a 1:1 thf solvate. [f] In Nujol. [g] Isolated as $[NBzEt_3]^+$ salt and analysed as a 2:1 CH_2Cl_2 solvate. [h] Analysed as a 1:1 CH_2Cl_2 solvate. [i] Analysed as a 2:1 CH_2Cl_2 solvate. [j] Also, ν(NO) at 1743s and ν(CN) at 2122w for the fragment (NC)Mn(PPh$_3$)(NO)(η-C$_5$H$_4$Me). [k] Isolated as $[PF_6]^-$ salt. [l] Also, ν(NO) at 1743s for the fragment (NC)Mn(PPh$_3$)(NO)(η-C$_5$H$_4$Me).

Table 2 Magnetic susceptibility, electrochemical and UV-visible spectroscopic data for $[Cl_2L'M(\mu\text{-}NC)MnL_x]^z$

Complex	L′	M	z	μ_{eff} [a]/μ_B	$E^{\circ\prime}$ [b]/V	λ_{max} [c]/nm (ε/dm^3 mol^{-1} cm^{-1})
1	thf	Co	0	4.3	0.32 [d]	672 (520), 655 (490), 625 (350), 574 (260), *ca.* 510 (180) [d]
2	thf	Mn	0	5.6	0.25 [d]	—
3	thf	Ni	0	3.3	0.26 [d]	—
5	Cl	Co	−1 [e]	—	0.11	—
6	Cl	Co	−1 [f]	4.5	0.12	671 (810), 650 (740), 616 (480), 601 (280)
7	Cl	Mn	−1 [f]	6.0	0.10	—
8	Cl	Ni	−1 [f]	—	0.09	—
9	4,4′-bipy	Co	0	—	0.28(I) (0.08 [g])	—
10	(NC)Mn(PPh$_3$)-(NO)(η-C$_5$H$_4$Me)	Co	0	—	0.17, 1.03	—
12	Cl	Co	0	4.6	0.11	677 (520), 650 (570), 633 (520), 609 (620), 600 (570), 513 (1130)
13	Cl	Mn	0	5.8	0.13	—
14	Cl	Ni	0	—	0.08	—

[a] At room temperature. [b] Reversible oxidation wave in cyclic voltammogram at platinum disk electrode in CH_2Cl_2 unless otherwise stated; I = irreversible. [c] In CH_2Cl_2 unless stated otherwise. [d] In thf. [e] $[NBzEt_3]^+$ salt. [f] $[PPN]^+$ salt. [g] Wave due to the uncomplexed ligand *trans*-[Mn(CN)(CO)(dppm)$_2$].

Each of the bimetallic complexes **1**–**10** shows one IR carbonyl band, at a higher energy than that of the free ligand *trans*-[Mn(CN)(CO)(dppm)$_2$] (CH_2Cl_2: ν(CO) = 1861s, ν(CN) = 2080mw cm^{-1}; thf: ν(CO) = 1866s, ν(CN) = 2083w cm^{-1}) but with no significant dependence on the identity of the tetrahedral metal centre M. On cyanide bridge formation, the intensity of ν(CN) increases as, in general, does the energy. However, given the balance between the kinematic effect of *N*-coordinating *trans*-[Mn(CN)(CO)(dppm)$_2$] to M, which acts to constrain the motion of the CN bond thus causing an increase in energy of ν(CN),[16] and the electronic effect, where a π-acidic (or electron withdrawing) metal fragment reduces the energy of ν(CN) by increasing Mn dπ to CN π* back-donation, complex **2** shows a small decrease in ν(CN). More significant, however, is the dependence on M of ν(CN) for a given set of analogous complexes. For each set, *e.g.* **1**–**3** and **5**–**8** (and also **12**–**14**, see below), ν(CN) increases in energy in the order M = Mn < Co < Ni (*e.g.* 2077, 2086 and 2098 cm^{-1} for **2**, **1** and **3** respectively). The small mass increase from Mn to Ni renders it unlikely that the kinematic effect alone causes the increase in energy of ν(CN). However, the order approximately reflects the electronegativities and ionic radii of the three metals, and is mirrored in the M–N bond lengths (see below).

Voltammetric studies

In thf, each of the complexes **1**–**3** shows a reversible diffusion-controlled one-electron oxidation wave, at *ca.* 0.30 V (Table 2), assigned to the one-electron oxidation of the Mn(I) centre to Mn(II); complexes **5**–**8** show similar waves in CH_2Cl_2. By contrast, complex **9** shows an incompletely reversible wave centred at 0.28 V, accompanied by a product wave at 0.08 V which is most likely due to the couple *trans*-$[Mn(CN)(CO)(dppm)_2]^+$/*trans*-[Mn(CN)(CO)(dppm)$_2$]. The implication that oxidation of **9** leads to decomposition of the product, $\mathbf{9}^+$, was confirmed by the IR spectrum of a 1:1 mixture of **9** and $[Fe(\eta\text{-}C_5H_5)_2][PF_6]$ in CH_2Cl_2 which showed ν(CO) and ν(CN) bands corresponding to the free ligand *trans*-$[Mn(CN)(CO)(dppm)_2]^+$. Finally, complex **10** not only shows an oxidation wave at 0.17 V, corresponding to the formation of the octahedral Mn(II) centre, but also a second reversible wave, at 1.03 V, corresponding to the oxidation of the pseudo-tetrahedral Mn(I) centre {*cf.* the $E^{\circ\prime}$ values of 0.07 and 0.83 V for *trans*-[Mn(CN)(CO)(dppm)$_2$] and $[Mn(CN)(PPh_3)(NO)(\eta\text{-}C_5H_4Me)]$ respectively}.

Chemical oxidation reactions

The 1:1 reaction in CH_2Cl_2 of **6** with the one-electron oxidant $[Fe(\eta\text{-}C_5H_5)(\eta\text{-}C_5H_4COMe)][BF_4]$, or of **7** or **8** with $[Fe(\eta\text{-}C_5H_5)_2][PF_6]$, in CH_2Cl_2 rapidly gave the neutral complexes $[Cl_3M(\mu\text{-}NC)MnL_x]$ {M = Co (**12**), Mn (**13**) and Ni (**14**)} (Tables 1 and 2). The IR spectra of **12**–**14** show increases in both ν(CN) and ν(CO) compared with those of **6**–**8**; the large shift in ν(CO) (*ca.* 70–75 cm^{-1}) and the somewhat smaller shift in ν(CN) (*ca.* 30 cm^{-1}) are consistent with one-electron oxidation at the octahedral Mn(I) centre. Each of **12**–**14** shows a reversible one-electron reduction wave at a potential essentially identical to that for the oxidation of the analogous Mn(I) anions **6**–**8**.

The UV-visible spectrum of the Mn(II) complex $[Cl_3Co(\mu\text{-}NC)MnL_x]$ **12** in CH_2Cl_2 is essentially a superimposition of the spectra of the analogous Mn(I) complex **6** and *trans*-$[Mn(CN)(CO)(dppm)_2]^+$ with very little change in the energies of the cobalt(II) absorptions. These results suggest that the cationic Mn(II) ligand *trans*-$[Mn(CN)(CO)(dppm)_2]^+$ has a similar ligand field strength to that of the Mn(I) ligand *trans*-[Mn(CN)(CO)(dppm)$_2$].

The room temperature magnetic moments of **12** and **13** are surprisingly similar to those of the anionic Mn(I) complexes **6** and **7**, *i.e.* they are lower than expected for complexes containing isolated low spin Mn(II) and tetrahedral M(II) centres. For example, the expected room temperature magnetic moment of **12** is *ca.* 4.9 μ_B $[(4.5^2 + 1.73^2)^{1/2}]$ but the observed moment is 4.6 μ_B. However, such differences are rather small and more detailed, variable temperature, magnetic susceptibility studies of **6** and **12** are required to study the possibility of some spin-pairing between the Mn(II) and M(II) paramagnetic centres *via* the cyanide bridge.

Complex **10** is also oxidised, using one equivalent of $[Fe(\eta\text{-}C_5H_5)_2][PF_6]$ in CH_2Cl_2, to give a deep blue solution which shows an IR spectrum consistent with the formation of the mixed-valence complex *trans*-$[Cl_2Co^{II}\{(\mu\text{-}NC)Mn^{II}L_x\}\{(\mu\text{-}NC)Mn^{I}(PPh_3)(NO)(\eta\text{-}C_5H_4Me)\}]^+$ **15** (Table 1). That ν(CO) increases in energy from 1876 to 1946 cm^{-1} while ν(NO) remains unchanged indicates trapped valence (or perhaps Class II) behaviour for **15**, with oxidation at the octahedral Mn(I) centre as suggested by the cyclic voltammetry of **10**; ν(CN) also increases in energy on oxidation. Attempts to isolate an analytically pure sample of **15** proved unsuccessful, preventing further detailed characterisation.

Structures of 1–3, 11 and 13

Crystals of **1** and of **2** and **3** as solvates, suitable for single crystal X-ray diffraction studies, were obtained by allowing a concentrated thf solution of each complex to diffuse into *n*-hexane at room temperature; those of **13**, as the CH_2Cl_2 solvate, were grown from CH_2Cl_2–*n*-hexane at −10 °C. During attempts to crystallise **6**, by layering a concentrated CH_2Cl_2 solution of the salt under *n*-hexane, small amounts of

Table 3 Selected bond lengths (Å) and angles (°) for $[Cl_2(thf)M(\mu\text{-}NC)MnL_x]$ (M = Co **1**, Mn **2** or Ni **3**), $[Cl_2Co\{(\mu\text{-}NC)MnL_x\}_2]$ **11** and $[Cl_3Mn(\mu\text{-}NC)MnL_x]$ **13**

	1	**2**	**3**	**11**	**13**
M–O	2.004(3)	2.153(3)[a]	2.026(3)	—	—
$M–Cl_{av}$	2.239(3)	2.316(3)	2.230(2)	2.274(2)	2.341(2)
M–N	1.970(3)	2.071(2)	1.953(3)	1.991(2)	2.138(4)
C–N	1.169(5)	1.162(3)	1.162(5)	1.167(3)	1.150(6)
Mn–C(N)	1.960(4)	1.950(2)	1.959(4)	1.986(3)	1.970(5)
Mn–C(O)	1.791(4)	1.794(2)	1.794(4)	1.792(3)	1.808(5)
$Mn–P(dppm)_{av}$	2.277(3)	2.286(2)	2.290(2)	2.286(2)	2.345(2)
N–M–Cl	112.0(2), 112.0(2)	114.5(2), 111.0(2)	109.3(2), 108.0(2)	113.2(2)	115.7(1), 104.2(1), 98.0(1)
Cl–M–Cl	114.0(2)	122.7(3)	132.5(6)	107.5(2)	116.0(1), 111.6(1), 109.7(1)
Mn–C–N	172.3(3)	179.8(2)	177.8(3)	177.4(2)	174.9(4)
N–M–O	103.0(2)	98.9(2)	97.9(2)	—	—
O–M–Cl	109.5(2), 105.6(2)	107.7(2),[a] 97.5(2)[a]	104.9(2), 97.8(2)	—	—
M–N–C	162.0(3)	155.4(2)	162.0(3)	167.0(2)	163.4(4)

[a] There is disorder involving one thf and one chloride ligand; the geometry for the major image is given.

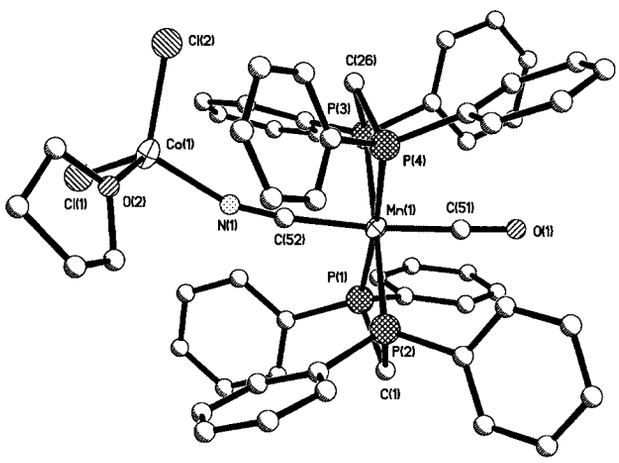

Fig. 1 The molecular structure of **1**. Hydrogen atoms have been omitted for clarity.

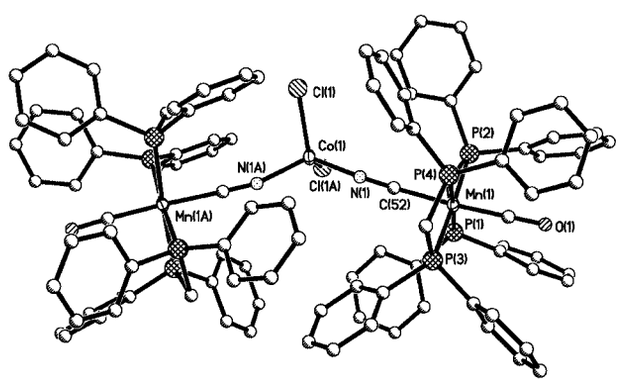

Fig. 2 The molecular structure of **11**. Hydrogen atoms have been omitted for clarity.

$[Cl_2Co\{(\mu\text{-}NC)MnL_x\}_2]$ **11** were fortuitously obtained. {As noted above, it proved impossible to prepare this complex directly from the 2:1 reaction of *trans*-$[Mn(CN)(CO)(dppm)_2]$ and $CoCl_2{\cdot}6H_2O$.} Its structure has also been determined. The structure of **1**, as a representative example of **1**–**3**, is shown in Fig. 1 and those of **11** and **13** are shown in Figs. 2 and 3 respectively. Selected structural data are given in Table 3.

The molecular structures of **1**–**3**, **11** and **13** are similar in comprising a *trans*-$[Mn(CN)(CO)(dppm)_2]$ unit of distorted octahedral geometry *N*-bound to the metal centre, M, with nearly linear Mn–C–N bonds but C–N–M bonds distorted from 180° by between 13 and 25° (see Table 3); these distortions are discussed further below. The average Mn–P distances for **1**–**3** and **11** are similar to those found in the free complex *trans*-

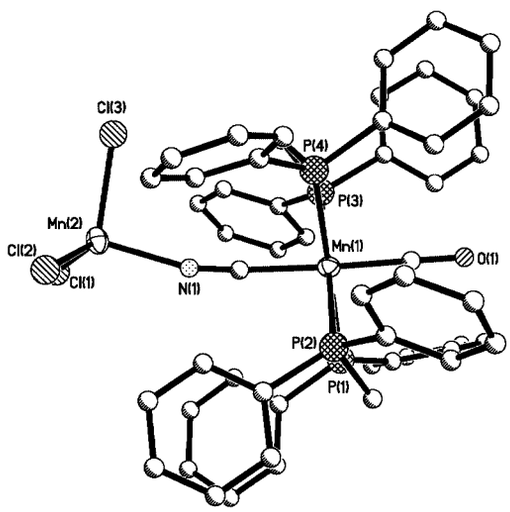

Fig. 3 The molecular structure of **13**. Hydrogen atoms have been omitted for clarity.

$[Mn(CN)(CO)(dppm)_2]$ and are therefore consistent with oxidation state Mn^I for the complexed cyanomanganese ligand. The presence of octahedral Mn(II) in complex **13**, implied by the spectroscopic and electrochemical data noted above, is shown most obviously by the Mn–P bond lengths which are closer to those in the Mn(II) complex *trans*-$[Mn(CN)(CO)(dppm)_2]^+$ than the Mn(I) analogue *trans*-$[Mn(CN)(CO)(dppm)_2]$.[5]

The cobalt atom of **1** has a slightly distorted tetrahedral geometry; the N–Co–Cl and Cl–Co–Cl angles are between 112.0(2)° and 114.0(2)°. There are more marked distortions in the tetrahedral geometry around the Mn(II) centre of **2** and the Ni(II) centre in **3** with the most distorted angles Cl–M–Cl {M = Mn, 122.7(3); M = Ni, 132.5(6)°}. The M–Cl distances are typical for each metal, M, in oxidation state II[17] with average M–Cl distances being 2.316(3), 2.239(3) and 2.230(2) for M = Mn, Co and Ni respectively. A similar trend is seen for the average M–N(C) distances, and is consistent with the ionic radii of the three metals which decrease in the order Mn(II) (0.80 Å) > Co(II) (0.72 Å) > Ni(II) (0.69 Å).[18] However, it is not clear why the Ni–O bond length of 2.026(3) Å should be *ca*. 0.02 Å longer than that of Co–O (but see below). The geometry at the tetrahedral manganese in **2** is rendered somewhat less reliable due to a disorder involving the thf and one chloride ligand. Complex **11** has C_2 symmetry with the cobalt atom, which lies on the two-fold axis, having a slightly distorted tetrahedral geometry and an N–Co–Cl angle of 113.2(2)°.

The geometry about the tetrahedral Mn(II) centre in **2** and **13** is affected by the ligand set. Thus the manganese atom of **2** is

coordinated to two chloride ligands and one thf molecule and has Cl–Mn–Cl 122.7(3)° whereas it is bound to three chloride ligands in **13** which shows average Cl–Mn–Cl 112.4°. Indeed the average Cl–M–Cl angles in all of **1**–**3**, **11** and **13** are over 109.5° while all the O–M–Cl or O–M–N angles are ≤109.5°. This is consistent with the poor electron donating ability of thf and therefore its weak binding to M. As a consequence the geometry at M is intermediate between truly tetrahedral and trigonal (*i.e.* that in which the thf is absent) albeit much closer to tetrahedral. In **1**–**3** (and most clearly for **3**) the Cl–M–Cl angle is the largest of the coordination angles at the 'tetrahedral' centre.

As we have noted previously for related Mn–CN–M systems, the C–N–M angle is much more flexible than the Mn–C–N angle and deviates much more dramatically from 180° in **1**–**3** and **13**. In these cases it seems likely that the direction of deviation is determined largely by the orientation of the tetrahedral metal centre relative to the four pseudo-axial phenyl groups on the proximal face of the $Mn(dppm)_2$ moiety (see Figs. 1 and 3). Thus, in each of **1**–**3**, one chloride ligand at M is interdigitated between two phenyl groups of one dppm ligand while the other two ligands at M (thf and Cl for **1**–**3**, and two Cl ligands in the case of **13**) are nearly eclipsed by the phenyl group at the second dppm. In order to alleviate the resultant steric clashes on this side of the complex the $MCl_2(thf)$ or other fragment is then tilted by the reduction of the C–N–M bond angle, leading to the observed deviation from linearity at N.

Conclusion

The reaction of *trans*-$[Mn(CN)L_x]$ $\{L_x = (CO)(dppm)_2\}$ with MCl_2 (M = Mn, Co or Ni) gives the bimetallic species $[Cl_2(thf)M(\mu\text{-}NC)MnL_x]$, the steric bulk of the monocarbonyl cyanomanganese(I) ligand preventing the formation of higher nuclearity complexes. However, thf displacement occurs with simple donors such as 4,4′-bipy and chloride ion and with the smaller cyanomanganese ligand $[Mn(CN)(PPh_3)(NO)(\eta\text{-}C_5H_4Me)]$. One-electron oxidation of complexes such as $[Cl_3M(\mu\text{-}NC)MnL_x]^-$ and $[Cl_2Co\{(\mu\text{-}NC)MnL_x\}\{(\mu\text{-}NC)Mn(PPh_3)(NO)(\eta\text{-}C_5H_4Me)\}]$ occurs at the octahedral Mn(I) centre of the $(NC)Mn(CO)(dppm)_2$ unit; magnetic susceptibility studies suggest that the two paramagnetic metal centres in $[Cl_3M^{II}(\mu\text{-}NC)Mn^{II}L_x]$ (M = Co or Mn) may weakly couple antiferromagnetically *via* the cyanide bridge; the UV-visible spectra of $[Cl_3Co(\mu\text{-}NC)Mn^{I}L_x]^-$ and $[Cl_3Co(\mu\text{-}NC)Mn^{II}L_x]$ suggest the ligand field strengths of the two ligands *trans*-$[Mn^{I}(CN)(CO)(dppm)_2]$ and *trans*-$[Mn^{II}(CN)(CO)(dppm)_2]^+$ are similar. Structural studies on $[Cl_2(thf)M(\mu\text{-}NC)MnL_x]$ (M = Mn, Co or Ni) and $[Cl_3Mn(\mu\text{-}NC)MnL_x]$ show that the M–N–C angle within the Mn(μ-CN)M bridge distorts so as to accommodate non-bonded interactions between the phenyl groups of the bulky $Mn(dppm)_2$ moiety and the ligands at the tetrahedral metal. Distortions from tetrahedral geometry at the M^{II} centres of $[Cl_2(thf)M(\mu\text{-}NC)MnL_x]$ may in part be related to the weak binding of thf.

Experimental

The preparation, purification and reactions of the complexes described were carried out under an atmosphere of dry nitrogen using dried, distilled and deoxygenated solvents; reactions were monitored by IR spectroscopy where necessary. Unless stated otherwise (i) complexes were purified by dissolution in CH_2Cl_2, filtration of the solution through Celite, addition of *n*-hexane to the filtrate and reduction of the volume of the mixture *in vacuo* to induce precipitation, and (ii) are stable under nitrogen and dissolve in polar solvents such as CH_2Cl_2, acetone and thf to give moderately air-stable solutions. The compounds *trans*-$[Mn(CN)(CO)(dppm)_2]$,[19] $[Mn(CN)(PPh_3)(NO)(\eta\text{-}C_5H_4Me)]$,[3,20] $[Fe(\eta\text{-}C_5H_5)_2][PF_6]$[21,22] and $[Fe(\eta\text{-}C_5H_5)(\eta\text{-}C_5H_4COMe)][PF_6]$[22] were prepared by published methods. IR spectra were recorded on a Nicolet 5ZDX FT spectrometer and UV-visible spectra on a Perkin-Elmer Lambda 2 UV/VIS spectrometer. Room temperature magnetic moments were determined using a Sherwood Mk I Magnetic Susceptibility Balance. Electrochemical studies were carried out as previously described.[5] Under the conditions used, $E^{\circ\prime}$ for the one-electron oxidation of $[Fe(\eta\text{-}C_5Me_5)_2]$ and $[Fe(\eta\text{-}C_5H_4COMe)_2]$, added to the test solutions as internal calibrants, are −0.08 and 0.97 V respectively in CH_2Cl_2, and 0.08 V ($[Fe(\eta\text{-}C_5Me_5)_2]$) in thf. Microanalyses were carried out by the staff of the Microanalytical Service of the School of Chemistry, University of Bristol.

Syntheses

$[Cl_2(thf)Co(\mu\text{-}NC)MnL_x]$ 1. To a stirred solution of $CoCl_2{\cdot}6H_2O$ (0.081 g, 0.34 mmol) in acetone (100 cm^3) was added *trans*-$[Mn(CN)(CO)(dppm)_2]$ (0.30 g, 0.34 mmol). After 15 min the green solution was filtered through Celite then evaporated to dryness *in vacuo*. The residue was extracted into thf (50 cm^3) and the solution filtered through Celite. A green powder was precipitated by the addition of *n*-hexane (100 cm^3) and reduction of the solvent volume *in vacuo*, yield 0.29 g (80%).

Crystals of $[Cl_2(thf)Co(\mu\text{-}NC)MnL_x]$ were grown by allowing a concentrated thf solution of the complex to diffuse into *n*-hexane at room temperature.

$[Cl_2(thf)Mn(\mu\text{-}NC)MnL_x]$ 2. The addition of *trans*-$[Mn(CN)(CO)(dppm)_2]$ (0.15 g, 0.17 mmol) to $MnCl_2$ (0.022 g, 0.17 mmol) dissolved in a mixture of EtOH (35 cm^3) and thf (20 cm^3) gave an orange suspension which dissolved when stirred for 15 min. The solution was filtered through Celite and then evaporated to dryness *in vacuo*. Dissolution of the orange residue in thf (15 cm^3) followed by the addition of *n*-hexane (15 cm^3) and reduction of the solvent volume *in vacuo* gave an orange powder, yield 0.13 g (71%).

Crystals of $[Cl_2(thf)Mn(\mu\text{-}NC)MnL_x]{\cdot}thf$ were grown by allowing a concentrated thf solution of the complex to diffuse into *n*-hexane at room temperature.

$[Cl_2(thf)Ni(\mu\text{-}NC)MnL_x]{\cdot}thf$, 3·thf. The addition of thf (25 cm^3) and then solid *trans*-$[Mn(CN)(CO)(dppm)_2]$ (0.202 g, 0.23 mmol) to a solution of $NiCl_2{\cdot}6H_2O$ (0.055 g, 0.23 mmol) in EtOH (40 cm^3) gave an orange-brown solution which was stirred for 15 min then evaporated to dryness *in vacuo*. The residue was extracted into thf (25 cm^3) to give an orange-brown solution which was filtered through Celite. Addition of *n*-hexane (20 cm^3) and reduction of the solvent volume *in vacuo* gave a brown powder, yield 0.14 g (56%).

Crystals of $[Cl_2(thf)Ni(\mu\text{-}NC)MnL_x]{\cdot}thf$ were grown by allowing a concentrated thf solution of the complex to diffuse into *n*-hexane at room temperature.

$[PPN][Cl_3Co(\mu\text{-}NC)MnL_x]{\cdot}CH_2Cl_2$, [PPN][6]·$CH_2Cl_2$. To a suspension of $[Cl_2(thf)Co(\mu\text{-}NC)MnL_x]$ (0.15 g, 0.14 mmol) in CH_2Cl_2 (15 cm^3) was added [PPN]Cl (0.09 g, 0.14 mmol). The solution was stirred for 5 min then filtered through Celite and evaporated to dryness *in vacuo*. The residue was washed with toluene (2 × 30 cm^3). Dissolution of the residue in CH_2Cl_2 (10 cm^3) followed by the addition of *n*-hexane (10 cm^3) and reduction of the solvent volume *in vacuo* gave a pale green powder, yield 0.16 g (73%).

The complex $[NEt_3Bz][Cl_3Co(\mu\text{-}NC)MnL_x]{\cdot}0.5CH_2Cl_2$, $[NEt_3Bz]$[**5**]·$0.5CH_2Cl_2$ was prepared similarly, using $[NEt_3Bz]Cl$ in place of [PPN]Cl.

$[PPN][Cl_3Mn(\mu\text{-}NC)MnL_x]$, [PPN][7]. The addition of [PPN]Cl (24 mg, 0.04 mmol) to $[Cl_2(thf)Mn(\mu\text{-}NC)MnL_x]$ (40 mg, 0.04 mmol) in CH_2Cl_2 (15 cm^3) gave a bright orange

Table 4 Crystal and refinement data for **1**, **2**·thf, **3**·thf, **11** and **13**·CH_2Cl_2

Compound	**1**	**2**·thf	**3**·thf	**11**	**13**·CH_2Cl_2
Formula	$C_{56}H_{52}Cl_2CoMnNO_2P_4$	$C_{60}H_{60}Cl_2Mn_2NO_3P_4$	$C_{60}H_{60}Cl_2MnNNiO_3P_4$	$C_{104}H_{88}Cl_2CoMn_2N_2O_2P_8$	$C_{53}H_{46}Cl_5Mn_2NOP_4$
Formula weight	1079.72	1147.83	1151.59	1885.38	1124.00
Crystal system	Triclinic	Triclinic	Triclinic	Monoclinic	Monoclinic
Space group (no.)	$P\bar{1}$ (2)	$P\bar{1}$ (2)	$P\bar{1}$ (2)	$C2/c$ (15)	$P2_1/c$ (14)
a/Å	10.192(2)	13.395(2)	13.371(1)	21.332(3)	12.629(3)
b/Å	13.922(2)	14.366(2)	14.325(2)	11.742(2)	23.525(4)
c/Å	19.286(4)	16.995(4)	17.179(2)	37.409(4)	18.306(4)
α/°	91.22(2)	110.09(1)	111.38(1)		
β/°	97.58(2)	106.83(1)	106.91(1)	92.52(2)	104.31(2)
γ/°	105.84(1)	99.21(1)	98.73(1)		
V/Å^3	2604.8(9)	2814.6(4)	2806.2(6)	9361(2)	5270(2)
Z	2	2	2	4	4
μ/mm^{-1}	0.827	0.702	0.815	0.915	0.893
Reflections collected	16491	17706	17900	21388	25042
Independent reflections	11361 [R_{int} = 0.0362]	11037 [R_{int} = 0.0162]	10285 [R_{int} = 0.0511]	8178 [R_{int} = 0.0340]	8253 [R_{int} = 0.050]
Final R_1 [$I > 2\sigma(I)$]	0.0582	0.0363	0.0657	0.0383	0.0521

solution which was stirred for 15 min then filtered through Celite. *n*-Hexane (15 cm^3) was added and the solvent volume reduced *in vacuo* to give an orange powder which was dried *in vacuo* for 1 h, yield 50 mg (81%).

[PPN][$Cl_3Ni(\mu$-NC)MnL_x]·0.5CH_2Cl_2, [PPN][8]·0.5CH_2Cl_2. To a solution of [PPN]Cl (61 mg, 0.093 mmol) in CH_2Cl_2 (50 cm^3) was added [Cl_2(thf)Ni(μ-NC)MnL_x] (100 mg, 0.093 mmol). The green solution was stirred for 20 min then filtered through Celite. The solvent volume was reduced *in vacuo* and then a mixture of *n*-hexane–diethyl ether (4:1) was added to give a green solid which was washed thoroughly with diethyl ether (2 × 20 cm^3) and dried, yield 110 mg (72%).

[Cl_2(4,4′-bipy)Co(μ-NC)MnL_x] 9. The addition of 4,4′-bipyridine (6 mg, 0.04 mmol) to a suspension of [Cl_2(thf)-Co(μ-NC)MnL_x] (40 mg, 0.04 mmol) in CH_2Cl_2 (15 cm^3) gave a green solution which was stirred for 10 min. The slightly turbid solution was then filtered through Celite, *n*-hexane (15 cm^3) was added and the solvent volume was reduced *in vacuo* to give a green powder, yield 30 mg (66%).

[Cl_2Co{(μ-NC)MnL_x}{(μ-NC)Mn(PPh_3)(NO)(η-C_5H_4Me)}]·0.5CH_2Cl_2, 10·0.5CH_2Cl_2. The addition of [Mn(CN)(PPh_3)-(NO)(η-C_5H_4Me)] (16 mg, 0.035 mmol) to a suspension of [Cl_2(thf)Co(μ-NC)MnL_x] (35 mg, 0.035 mmol) in CH_2Cl_2 (20 cm^3) gave a green solution which was stirred for 10 min. The solution was filtered through Celite, then *n*-hexane (15 cm^3) was added and the solvent volume was reduced *in vacuo* to give an oily green solid which was dried *in vacuo*, yield 27 mg (53%).

[Cl_3Co(μ-NC)MnL_x] 12. The addition of [Fe(η-C_5H_5)(η-C_5H_4COMe)][BF_4] (14 mg, 0.045 mmol) to [PPN][Cl_3Co-(μ-NC)MnL_x] (75 mg, 0.045 mmol) in CH_2Cl_2 (10 cm^3) gave a red-brown solution which was stirred for 5 min then filtered through Celite. Addition of *n*-hexane (10 cm^3) and reduction of the solvent volume *in vacuo* gave a purple powder which was filtered off in air, washed with *n*-hexane (2 × 30 cm^3), then dried *in vacuo* for 1 h, yield 40 mg (85%).

[Cl_3Mn(μ-NC)MnL_x]·CH_2Cl_2 13. The addition of CH_2Cl_2 (30 cm^3) and [Cl_2(thf)Mn(μ-NC)MnL_x] (190 mg, 0.18 mmol) and [PPN]Cl (120 mg, 0.18 mmol) gave an orange suspension which, when stirred for 15 min, gave an orange solution. Addition of [Fe(η-C_5H_5)$_2$][PF_6] (60 mg, 0.18 mmol) and then stirring the mixture for a further 15 min gave a red solution which was filtered through Celite. The volume of the filtrate was reduced *in vacuo* (by *ca*. 10 cm^3) and then *n*-hexane was added to give dark red powder, yield 140 mg (70%).

Deep red crystals of [Cl_3Mn(μ-NC)MnL_x]·CH_2Cl_2 were grown by allowing a dilute solution of the complex in CH_2Cl_2 to diffuse into *n*-hexane at −10 °C.

[Cl_3Ni(μ-NC)MnL_x]·0.5CH_2Cl_2, 14·0.5CH_2Cl_2. To a solution of [PPN][Cl_3Ni(μ-NC)MnL_x] (220 mg, 0.14 mmol) in CH_2Cl_2 (40 cm^3) was added [Fe(η-C_5H_5)$_2$][PF_6] (46 mg, 0.14 mmol). The red solution was stirred for 30 min then filtered through Celite, reduced in volume (to *ca*. 30 cm^3) and treated with diethyl ether (30 cm^3). The resulting dark red powder was removed by filtration and dried *in vacuo* for 24 h, yield 120 mg (77%).

Crystal structure determinations of 1, 2·thf, 3·thf, 11 and 13·CH_2Cl_2

Many of the details of the structure analyses of **1**, **2**·thf, **3**·thf, **11** and **13**·CH_2Cl_2 are presented in Table 4. A full hemisphere of reciprocal space was scanned with the area detector centre held at $2\theta = -27°$.

CCDC reference number 186/1917.

See http://www.rsc.org/suppdata/dt/b0/b001782p/ for crystallographic files in .cif format.

Acknowledgements

We thank the EPSRC for Research Studentships (to O. M. H., G. R. L. and A. J. W.).

References

1 G. A. Carriedo, V. Riera, N. G. Connelly and S. J. Raven, *J. Chem. Soc.*, *Dalton Trans.*, 1987, 1769.
2 N. G. Connelly, K. A. Hassard, B. J. Dunne, A. G. Orpen, S. J. Raven, G. A. Carriedo and V. Riera, *J. Chem. Soc.*, *Dalton Trans.*, 1988, 1623.
3 D. Bellamy, N. G. Connelly, O. M. Hicks and A. G. Orpen, *J. Chem. Soc.*, *Dalton Trans.*, 1999, 3185; M. Bardaji, N. C. Brown, N. G. Connelly, R. Davies, A. G. Orpen, G. M. Rosair and N. R. Seear, *J. Organomet. Chem.*, 1994, **474**, C21.
4 G. A. Carriedo, N. G. Connelly, S. Alvarez, E. Perez-Carreno and S. Garcia-Granda, *Inorg. Chem.*, 1993, **32**, 272.
5 G. A. Carriedo, N. G. Connelly, E. Perez-Carreno, A. G. Orpen, A. L. Rieger, P. H. Rieger, V. Riera and G. M. Rosair, *J. Chem. Soc.*, *Dalton Trans.*, 1993, 3103.
6 N. C. Brown, G. B. Carpenter, N. G. Connelly, J. G. Crossley, A. Martin, A. G. Orpen, A. L. Rieger, P. H. Rieger and G. H. Worth, *J. Chem. Soc.*, *Dalton Trans.*, 1996, 3977.
7 F. L. Atkinson, A. Christofides, N. G. Connelly, H. J. Lawson, A. C. Loyns, A. G. Orpen, G. M. Rosair and G. H. Worth, *J. Chem. Soc.*, *Dalton Trans.*, 1993, 1441.
8 F. L. Atkinson, N. C. Brown, N. G. Connelly, A. G. Orpen,

A. L. Rieger, P. H. Rieger and G. M. Rosair, *J. Chem. Soc.*, *Dalton Trans.*, 1996, 1959.
9 N. G. Connelly, O. M. Hicks, G. R. Lewis, A. G. Orpen and A. J. Wood, *Chem. Commun.*, 1998, 517.
10 G. N. Richardson and H. Vahrenkamp, *J. Organomet. Chem.*, 2000, **593–594**, 44.
11 O. M. Hicks, PhD Thesis, University of Bristol, 1997.
12 N. G. Connelly, G. R. Lewis, M. T. Moreno and A. G. Orpen, *J. Chem. Soc.*, *Dalton Trans.*, 1998, 1905.
13 F. A. Cotton, G. Wilkinson, C. A. Murillo and M. Bochmann, *Advanced Inorganic Chemistry*, Wiley-Interscience, New York, 1999, 6th edn., p. 821.
14 B. N. Figgis and J. Lewis, in *Modern Coordination Chemistry*, eds. J. Lewis and R. C. Wilkins, Interscience, New York, 1960, p. 406.
15 F. A. Cotton, G. Wilkinson, C. A. Murillo and M. Bochmann, *Advanced Inorganic Chemistry*, Wiley-Interscience, New York, 1999, 6th edn., p. 841.
16 D. A. Downs, A. Haim and W. K. Wilmarth, *J. Inorg. Nucl. Chem.*, 1961, **21**, 33.
17 *International Tables for Crystallography*, Kluwer, Dordrecht, 1992, vol. C.
18 *Encyclopedia of Inorganic Chemistry*, ed. R. B. King, Wiley, New York, vol. 2, p. 931.
19 A. Christofides, N. G. Connelly, H. J. Lawson, A. C. Loyns, A. G. Orpen, M. O. Simmonds and G. H. Worth, *J. Chem. Soc.*, *Dalton Trans.*, 1991, 1595.
20 D. L. Reger, D. J. Fauth and M. D. Dukes, *J. Organomet. Chem.*, 1979, **170**, 217.
21 J. C. Smart and B. L. Pinsky, *J. Am. Chem. Soc.*, 1980, **102**, 1009.
22 N. G. Connelly and W. E. Geiger, *Chem. Rev.*, 1996, **96**, 877.